Electronic Supplementary Material (ESI) for ChemComm.

Supporting Information

Chloride triggered reversible switching from a metallosupramolecular $[Pd_2L_4]^{4+}$ cage to a $[Pd_2L_2Cl_4]$ metallo-macrocycle with release of *endo*- and *exo*-hedrally bound guests

Dan Preston,[a] Alyssa Fox-Charles,[a] Warrick K. C. Lo[a] and James D. Crowley[a]*

[a]Department of Chemistry, University of Otago, PO Box 56, Dunedin,

New Zealand; Fax: +64 3 479 7906; Tel: +64 3 479 7731.

***jcrowley@chemistry.otago.ac.nz**

Contents

1 Experimental

1.1 Synthetic scheme

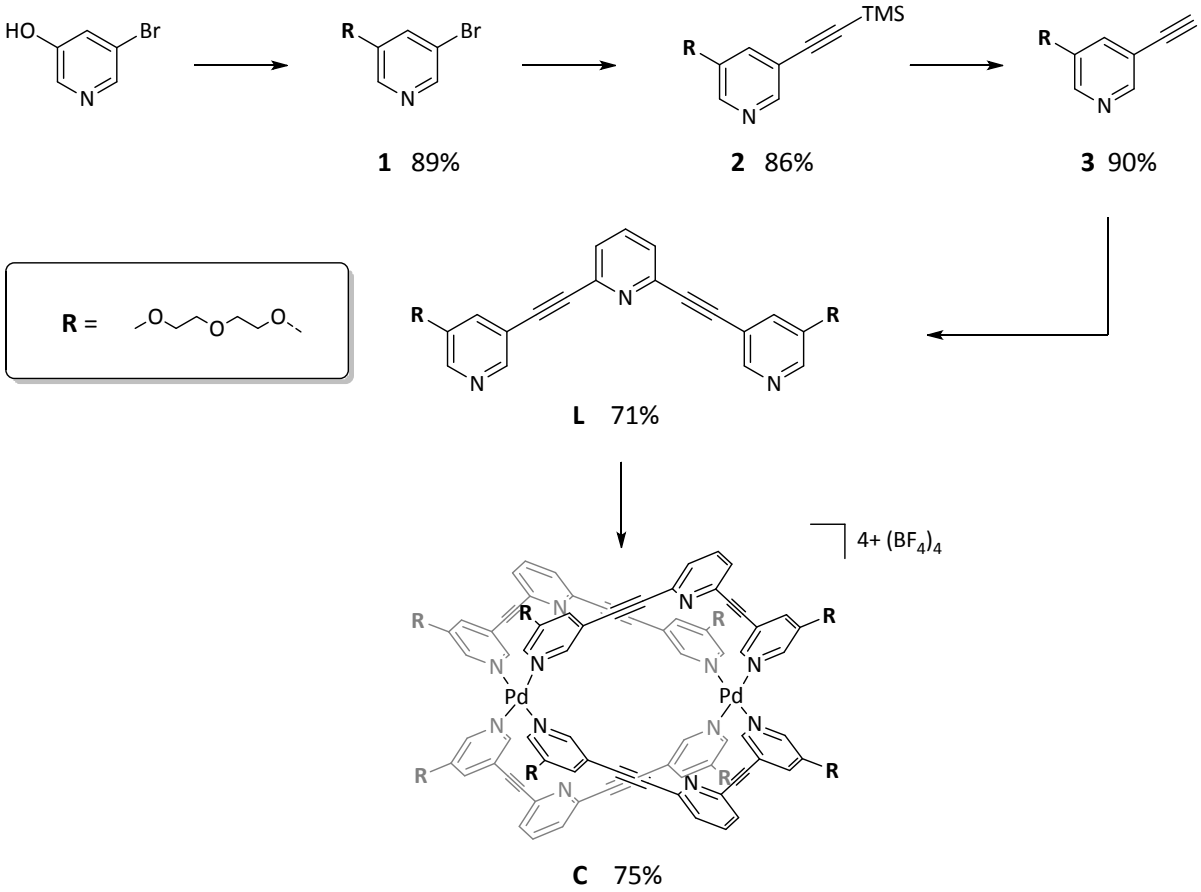

1.2 General

Unless otherwise stated, all reagents were purchased from commercial sources and used without further purification except 1-chloro-2-(2-methoxyethoxy)ethane which was synthesised according to a literature procedure.[1] Solvents were laboratory reagent grade. Petrol refers to the fraction of petroleum ether boiling in the range 40-60 °C. ^{1}H and ^{13}C NMR spectra were recorded on either a 400 MHz Varian 400-MR or Varian 500 MHz AR spectrometer. Chemical shifts (δ) are reported in parts per million (ppm) and referenced to residual solvent peaks ($CDCl_3$: ^{1}H δ 7.26 ppm, ^{13}C δ 77.16 ppm; CD_3CN: ^{1}H δ 1.94, ^{13}C δ 1.32, 118.26 ppm; d_6-DMSO: ^{1}H δ 2.50 ppm, ^{13}C δ 39.52 ppm). Coupling constants (*J*) are reported in Hertz (Hz). Standard abbreviations indicating multiplicity were used as follows: m = multiplet, q = quartet, t = triplet, dt = double triplet, d = doublet, dd = double doublet, s = singlet, br = broad. IR spectra were recorded on a Bruker ALPHA FT-IR spectrometer with an attached ALPHA-P measurement module. Microanalyses were performed at the Campbell Microanalytical Laboratory at the University of Otago. Electrospray mass spectra (HR-ESMS) were collected on a Bruker micrOTOF-Q spectrometer.

1.3 Synthesis of 1 ($C_{10}H_{14}BrNO_3$)

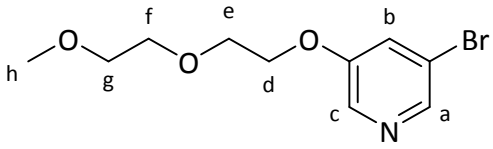

1-chloro-2-(2-methoxyethoxy)ethane[1] (4.82 g, 34.8 mmol, 1.5 eq.), 5-bromopyridin-3-ol (4.03 g, 23.2 mmol, 1 eq.) and K_2CO_3 (6.41 g, 46.4 mmol, 2 eq.) were dissolved in DMF (30 mL) and stirred overnight at 90 °C. After filtration the solvent was removed under vacuum. The residue was taken up in DCM (50 mL), washed with water (100 mL), with extraction of the aqueous layer with 3:1 $CHCl_3$/IPA (50 mL). The organic layers were combined, dried with Na_2SO_4 and filtered, before the solvent was removed under vacuum. Column chromatography on silica (DCM, then 1:19 acetone/DCM, then 1:4 acetone/DCM) gave the product as an orange oil. Yield = 5.72 g, 20.6 mmol, 89 %. ^{1}H NMR (400 MHz, $CDCl_3$, 298 K) δ: 8.28 (1H, d, *J* = 1.8 Hz, H_a), 8.26 (1H, d, *J* = 2.5 Hz, H_c), 7.40 (1H, t, *J* = 2.1 Hz, H_b), 4.19-4.16 (2H, m, H_d), 3.87-3.85 (2H, m, H_e), 3.72-3.69 (2H, m, H_f), 3.58-3.56 (2H, m, H_g), 3.39 (3H, s, H_h). ^{13}C NMR (100 MHz, $CDCl_3$, 298 K) δ: 155.1, 142.8 (C_a), 136.4 (C_c), 123.9 (C_b), 120.0, 71.7 (C_d), 70.6 (C_e), 69.2 (C_f), 68.0 (C_g), 58.8 (C_h). HR-ESMS ($CHCl_3$) *m/z* = 298.0027 [M + Na]$^+$ (calc. for $C_{10}H_{14}BrNNaO_3$, 298.0049), *m/z* = 276.0205 [M + H]$^+$ (calc. for $C_{10}H_{15}BrNO_3$, 276.0230). Anal. calcd. for $C_{10}H_{14}BrNO_3$·0.1acetone: C, 43.88; H, 5.22; N, 4.97%; found: C, 43.72; H, 5.28; N, 4.63%. IR: ν (cm^{-1}) 2877, 2106, 1741, 1573, 1554, 1428, 1310, 1261, 1220, 1135, 1105, 1051, 1007, 935, 856.

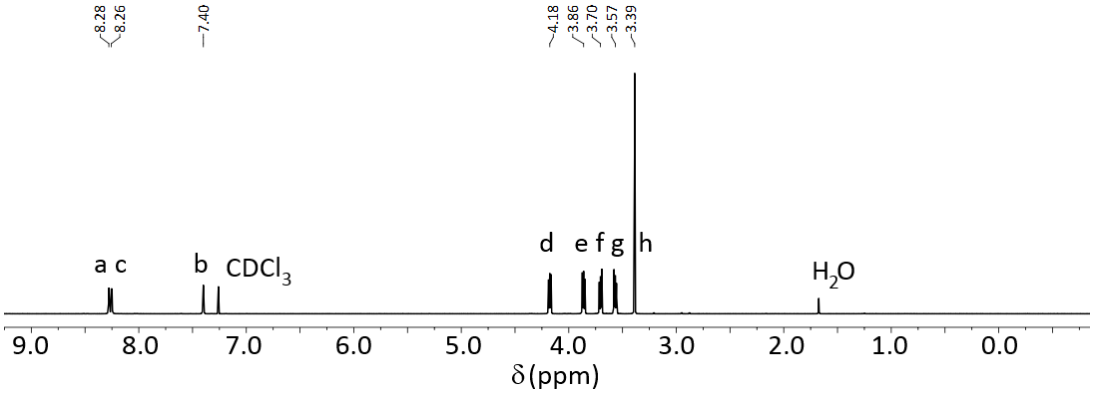

Figure 1.1 ^{1}H NMR spectrum (400 MHz, $CDCl_3$, 298K) of **1**.

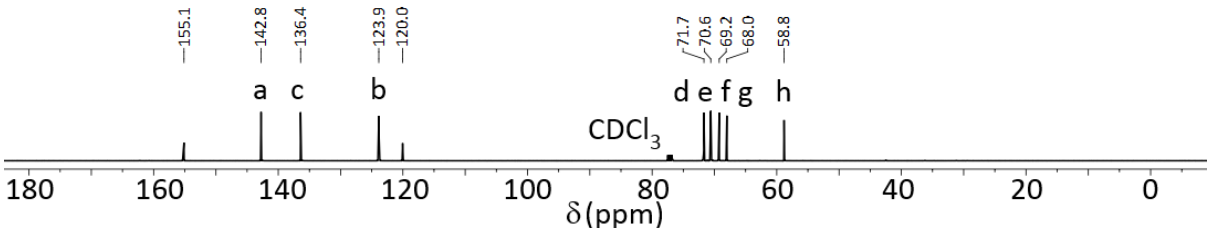

Figure 1.2 ^{13}C NMR spectrum (100 MHz, $CDCl_3$, 298K) of **1**.

1.4 Synthesis of 2 ($C_{15}H_{23}NO_3Si$)

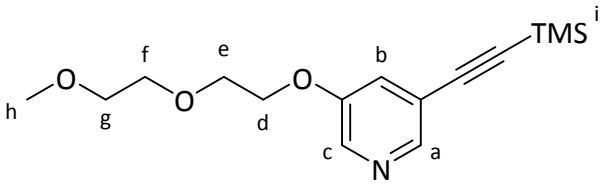

A solution of **1** (1.00 g, 3.62 mmol, 1 eq.) in diisopropylamine (6 mL) was degassed with N_2 for 15 minutes. Trimethylsilylacetylene (1.470 mL, 10.86 mmol, 3 eq.), $[Pd(PPh_3)_2]Cl_2$ (0.10 g, 0.15 mmol, 0.03 eq.) and copper(I) iodide (0.07 g, 0.36 mmol, 0.1 eq.) were added and the reaction mixture was heated at 70 °C for 2 days. A mixture of 3:1 $CHCl_3$/IPA (50 mL) and aqueous 0.1 M EDTA/NH_4OH solution (50 mL) were added and the mixture was stirred vigorously for 2 hours. After filtration through Celite and separation, the organic layer was washed with brine (100 mL), dried with $MgSO_4$ and the solvent was removed under vacuum. Column chromatography on silica (DCM, then 1:7 acetone/DCM) gave a brown oil. Yield = 0.92 g, 3.11 mmol, 86%. ^{1}H NMR (400 Hz, $CDCl_3$, 298 K) δ: 8.29 (1H, d, *J* = 1.6 Hz, H_c), 8.26 (1H, d, *J* = 1.8 Hz, H_a), 7.25 (1H, m, H_b), 4.18-4.16 (2H, m, H_d), 3.87-3.85 (2H, m, H_e), 3.72-3.70 (2H, m, H_f), 3.58-3.56 (2H, m, H_g), 3.39 (3H, s, H_h), 0.26 (9H, s, H_i). ^{13}C NMR (100 Hz, $CDCl_3$, 298 K) δ: 154.1, 144.9 (C_c), 138.1 (C_a), 123.1 (C_b), 120.2, 101.3, 97.8, 71.8 (C_d), 70.7 (C_e), 69.4 (C_f), 67.8 (C_g), 58.9 (C_h), -0.3 (C_i). HR-ESMS ($CHCl_3$/MeOH): *m/z* = 316.1332 $[M + Na]^+$ (calc. for $C_{15}H_{23}NNaO_3Si$, 316.1339), *m/z* = 294.1511 $[M + H]^+$ (calc. for $C_{15}H_{24}NO_3Si$, 294.1520). Anal. calcd. for $C_{15}H_{23}NO_3Si{\cdot}0.7H_2O$: C, 58.87; H, 8.04; N, 4.58%; found: C, 58.50; H, 7.85; N, 4.54%. IR: ν (cm^{-1}) 2958, 2925, 2159, 1581, 1419, 1290, 1249, 1171, 1108, 1058, 1019, 993, 840, 759, 701.

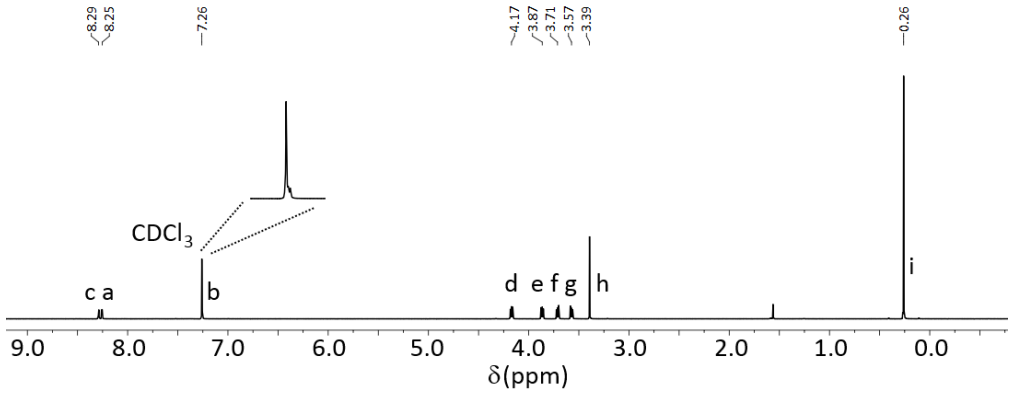

Figure 1.3 ^{1}H NMR spectrum (400 MHz, $CDCl_3$, 298K) of **2**.

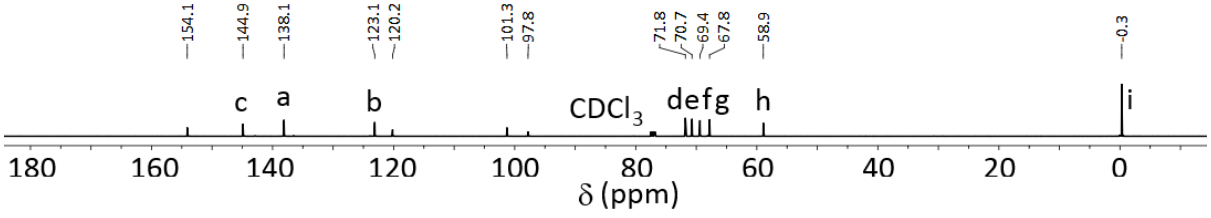

Figure 1.4 ^{13}C NMR spectrum (100 MHz, $CDCl_3$, 298K) of **2**.

1.5 Synthesis of 3 ($C_{12}H_{15}NO_3$)

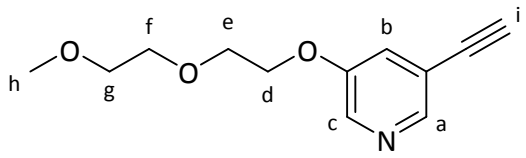

To a solution of **2** (0.917 g, 3.13 mmol, 1 eq.) in methanol (40 mL) was added Na_2CO_3 (0.663 g, 6.25 mmol, 2 eq.), and the mixture was stirred for 2 hours at RT. After filtration and removal of solvent under vacuum, the residue was purified through column chromatography on silica (DCM, then 1:10 acetone/DCM, then 1:3 acetone/DCM) to give a brown oil. Yield = 0.491 g, 2.50 mmol, 80%. ^{1}H NMR (400 MHz, $CDCl_3$, 298 K) δ: 8.28 (1H, d, *J* = 2.4 Hz, H_a), 8.26 (1H, d, *J* = 2.9 Hz, H_c), 7.26 (1H, m, H_b), 4.19-4.16 (2H, m, H_d), 3.88-3.85 (2H, m, H_e), 3.72-3.70 (2H, m, H_f), 3.58-3.56 (2H, m, H_g), 3.35 (3H, s, H_h), 3.18 (1H, s, H_i). ^{13}C NMR (100 MHz, $CDCl_3$, 298 K) δ: 154.3, 145.2 (C_a), 138.5 (C_c), 123.8 (C_b), 119.4, 80.5 (C_i), 80.3, 72.0 (C_d), 70.9 (C_e), 69.6 (C_f), 68.0 (C_g), 59.1 (C_h). HR-ESMS ($CHCl_3$): *m/z* = 244.09 $[M + Na]^+$ (calc. for $C_{12}H_{15}NNaO_3$, 244.09), *m/z* = 222.1110 $[M + H]^+$ (calc. for $C_{12}H_{16}NO_3$, 222.1125). Anal. calcd. for $C_{12}H_{15}NO_3$: C, 65.14; H, 6.83; N, 6.33%; found: C, 65.20; H, 6.94; N, 6.10%. IR: ν (cm^{-1}) 3226, 2875, 1580, 1560, 1420, 1319, 1285, 1170, 1106, 1056, 1018, 984, 873, 847, 700.

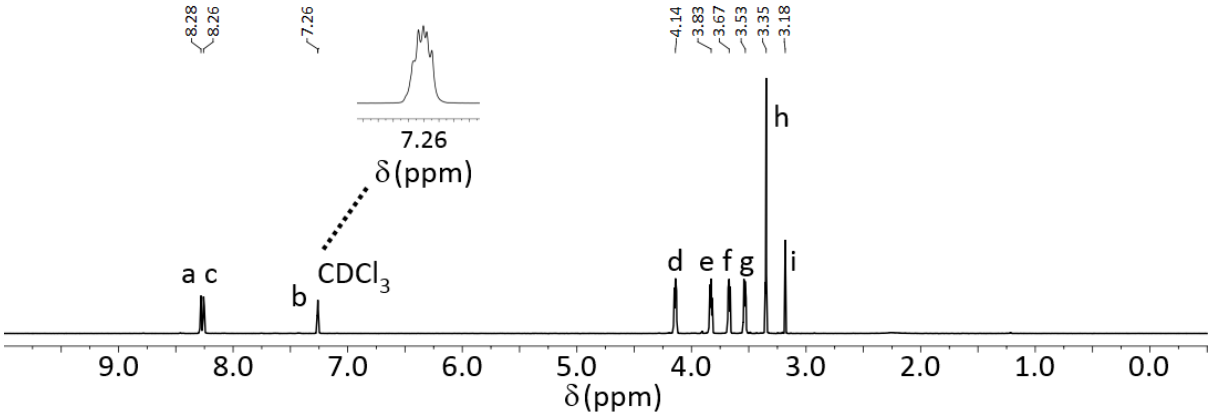

Figure 1.5 ^{1}H NMR spectrum (400 MHz, $CDCl_3$, 298K) of **3**.

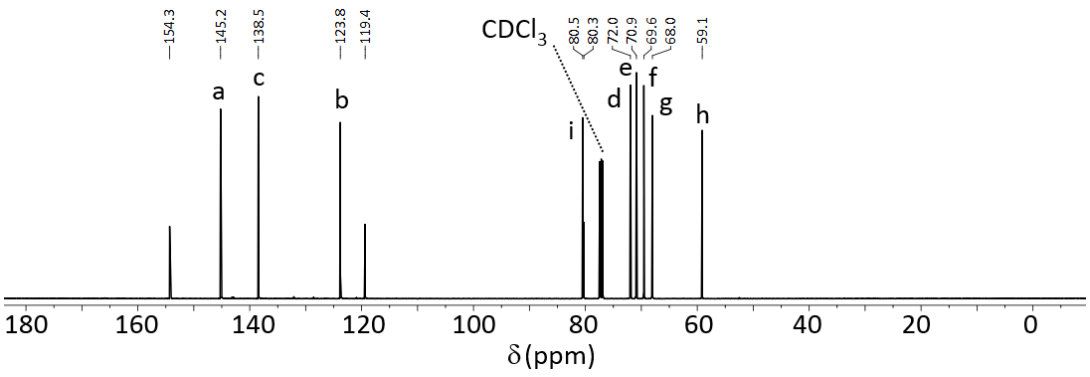

Figure 1.6 ^{13}C NMR spectrum (100 MHz, $CDCl_3$, 298K) of **3**.

1.6 Synthesis of L ($C_{29}H_{31}N_3O_6$)

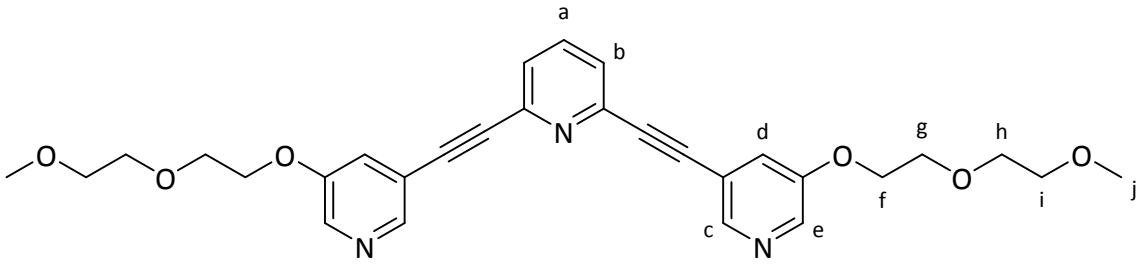

A solution of **3** (0.13 g, 0.59 mmol, 2 eq.) in diisopropylamine (25 mL) and THF (25 mL) was de-gassed with N_2 for 15 minutes, before addition of 2,6-dibromopyridine (0.07 g, 0.29 mmol, 1 eq.), $Pd(PPh_3)_2Cl_2$ (0.01 g, 0.02 mmol, 0.05 eq.) and copper(I) iodide (0.06 g, 0.03 mmol, 0.1 eq.), and the reaction was stirred under N_2 at room temperature for 2 days. Aqueous 0.1 M EDTA/NH_4OH solution (50 mL) and 3:1 $CHCl_3$/IPA (50 mL) were added and the solution was stirred for 2 hours. After filtration through Celite and separation, the organic layer was washed with brine (2 x 100 mL), dried with Na_2SO_4 and the solvent was removed under vacuum. Purification of the residue through column chromatography on silica (DCM, then 1:3 acetone/DCM, then 1:2 acetone/DCM) gave a colourless solid. Yield = 0.11 g, 209 mmol, 71%. ^{1}H NMR (400 MHz, $CDCl_3$, 298 K) δ: 8.39 (2H, d, *J* = 1.4 Hz, H_c), 8.31 (2H, d, *J* = 2.8 Hz, H_e), 7.83 (1H, t, *J* = 1.6 Hz, H_a), 7.60 (2H, d, *J* = 7.8 Hz, H_b), 7.51 (2H, dd, *J* = 2.7 & 1.5 Hz, H_d), 4.21-4.19 (4H, m, H_f), 3.90-3.88 (4H, m, H_g), 3.74-3.72 (4H, m, H_h), 3.60-3.58 (4H, m, H_i), 3.40 (6H, s, H_j). ^{13}C NMR (100 MHz, $CDCl_3$, 298 K) δ: 155.5, 145.5 (C_c), 143.9, 139.9 (C_e), 138.4 (C_a), 128.1 (C_b), 124.1 (C_d), 120.0, 91.4, 86.4, 72.6 (C_i), 71.2 (C_h), 70.0 (C_f), 69.2 (C_g), 58.9 (C_j). HR-ESMS: ($CHCl_3$/MeOH) *m/z* = 540.2093 $[M + Na]^+$ (calc. for $C_{29}H_{31}N_3NaO_6$, 540.2185), m/z = 518.2260 $[M + H]^+$ (calc. for $C_{29}H_{32}N_3O_6$, 518.2286). Anal. calcd. for $C_{29}H_{31}N_3O_6$: C, 67.30; H, 6.04; N, 8.12%, found: C, 67.15; H, 6.00; N, 7.98%. IR: ν (cm^{-1}) 3046, 2887, 2208, 1582, 1554, 1459, 1441, 1418, 1330, 1311, 1250, 1220, 1195, 1166, 1126, 1100, 1054, 1034, 1013, 981, 965, 912, 875, 821.

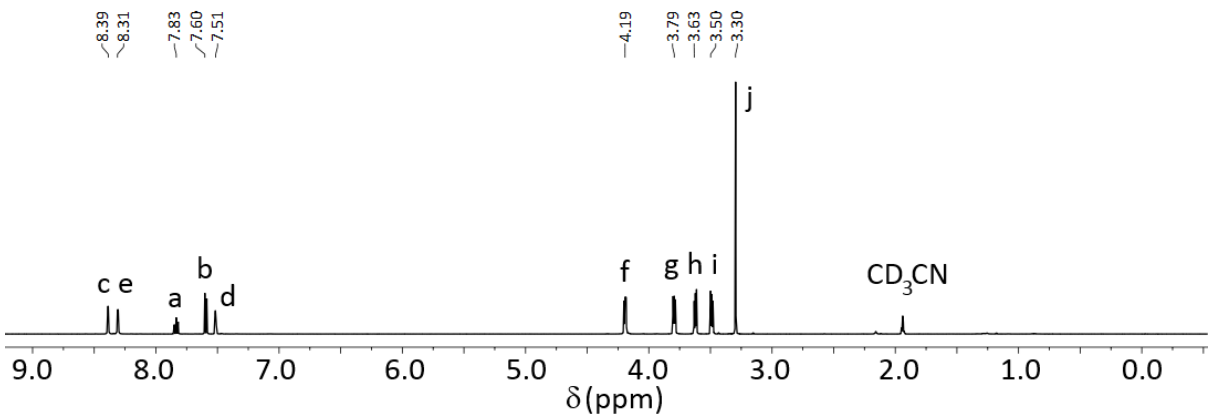

Figure 1.7 ^{1}H NMR spectrum (400 MHz, CD_3CN, 298K) of **L**.

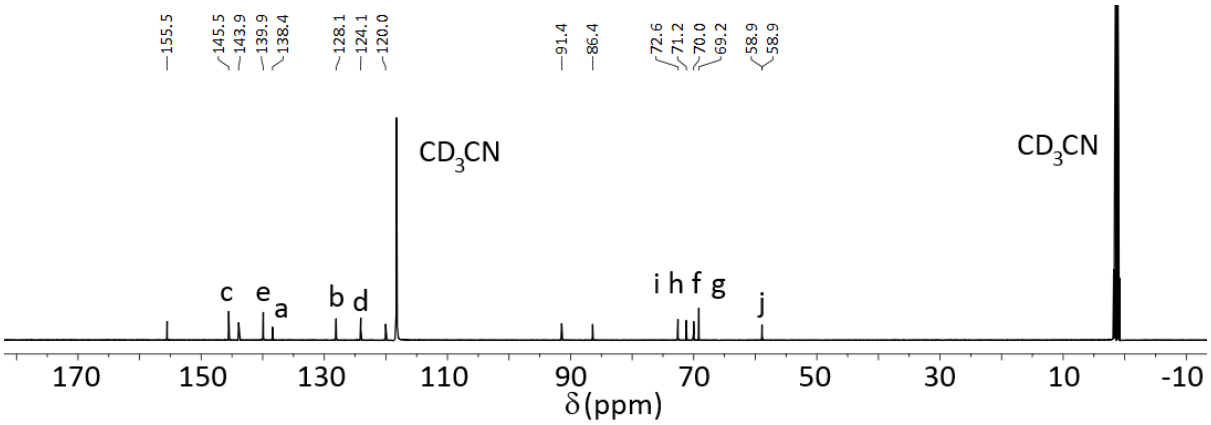

Figure 1.8 ^{13}C NMR spectrum (100 MHz, CD_3CN, 298K) of **L**.

1.7 Synthesis of C ($C_{116}H_{124}N_{120}O_{24}Pd_2B_4F_{16}$)

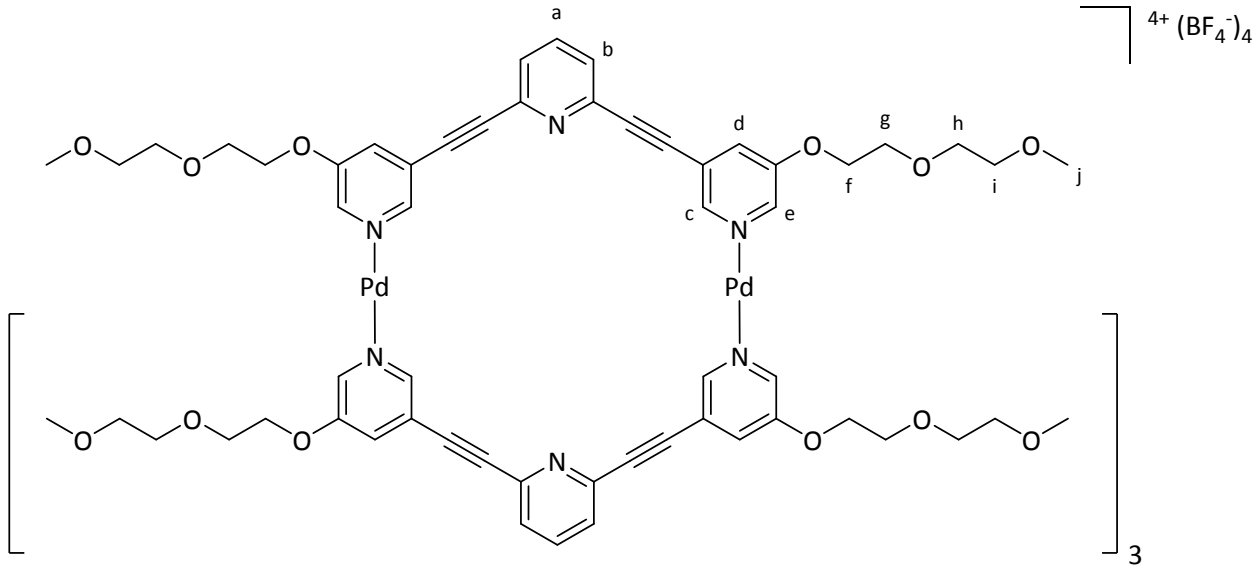

Combination of **L** (92.5 mg, 0.179 mmol, 4 eq.) and $[Pd(CH_3CN)_4](BF_4)_2$ (39.7 mg, 0.089 mmol, 2 eq.) in acetonitrile (5 mL) gave instantaneous product formation. The product was precipitated with diethyl ether to give a tan solid. Yield = 83 mg, 33 mmol, 75%. ^{1}H NMR (400 Hz, $CDCl_3$, 298 K) δ: 9.00 (2H, d, *J* = 1.2 Hz, H_c), 8.91 (2H, d, *J* = 2.6 Hz, H_e), 7.91 (1H, t, *J* = 3.2 Hz, H_a), 7.81 (2H, dd, *J* = 1.3 & 2.4 Hz, H_d), 7.72 (2H, d, *J* =7.8 Hz, H_b), 4.35-4.33 (4H, m, H_f), 3.86-3.85 (4H, m, H_g), 3.67-3.65 (4H, m, H_h), 3.53-3.51 (4H, m, H_i), 3.34 (6H, s, H_j). ^{13}C NMR (100 Hz, $CDCl_3$, 298 K) δ: 158.0, 146.1 (C_c), 143.3, 140.1 (C_e), 138.7 (C_a), 129.6 (C_d), 129.4 (C_b), 123.8, 94.2, 83.4, 72.5 (C_i), 71.2 (C_h), 70.5 (C_f), 69.7 (C_g), 58.9 (C_j). HR-ESMS (CD_3CN): *m/z* = 1228.3430 $[M - (BF_4)_2]^{2+}$ (calc. for $C_{116}H_{124}B_2F_8N_{12}O_{24}Pd_2$ 1228.3518), *m/z* = 789.8970 $[M - (BF_4)_3]^{3+}$ (calc. for $C_{116}H_{124}BF_4N_{12}O_{24}Pd_2$ 789.8998), *m/z* = 570.6726 $[M - (BF_4)_4]^{4+}$, (calc. for $C_{116}H_{124}N_{12}O_{24}Pd_2$ 570.6737). Anal. calcd. for $C_{116}H_{124}B_4F_{16}N_{12}O_{24}$ $Pd_2 \cdot 4H_2O$: C, 51.56; H, 4.92; N, 6.22%, found: C, 51.60; H, 5.04; N, 6.20%. IR: ν (cm^{-1}) 3083, 2882, 1583, 1559, 1437, 1328, 1246, 1165, 1052, 877.

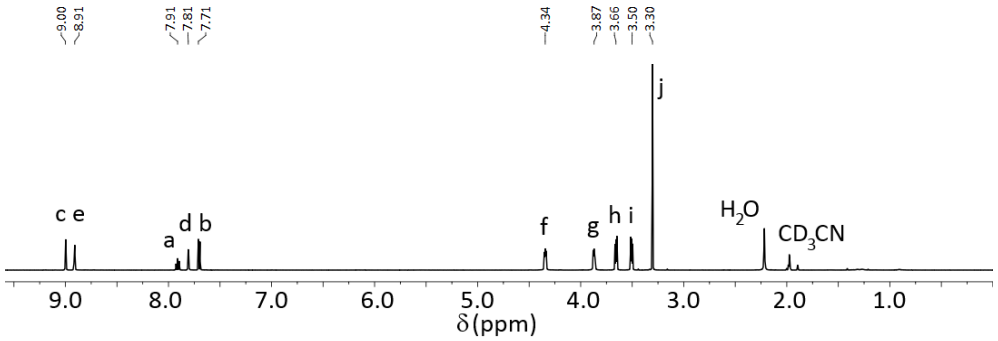

Figure 1.9 ^{1}H NMR spectrum (400 MHz, CD_3CN, 298K) of **C**.

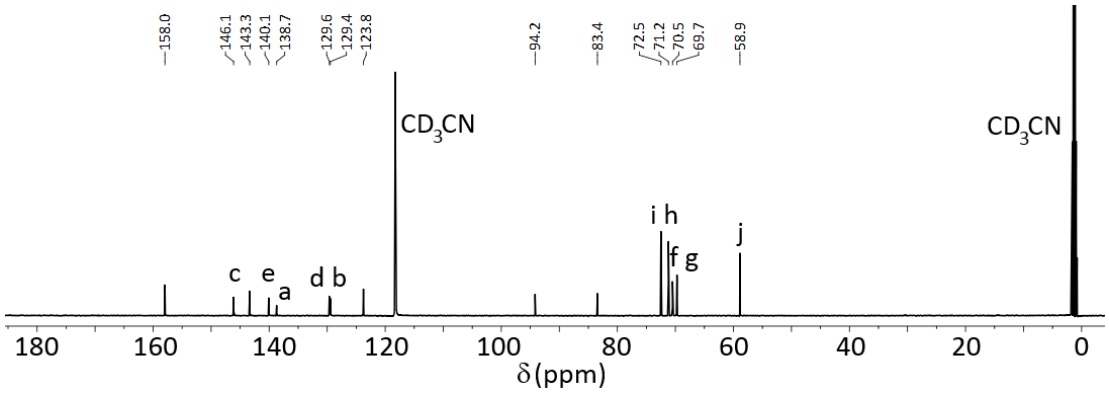

Figure 1.10 ^{13}C NMR spectrum (100 MHz, CD_3CN, 298K) of **C**.

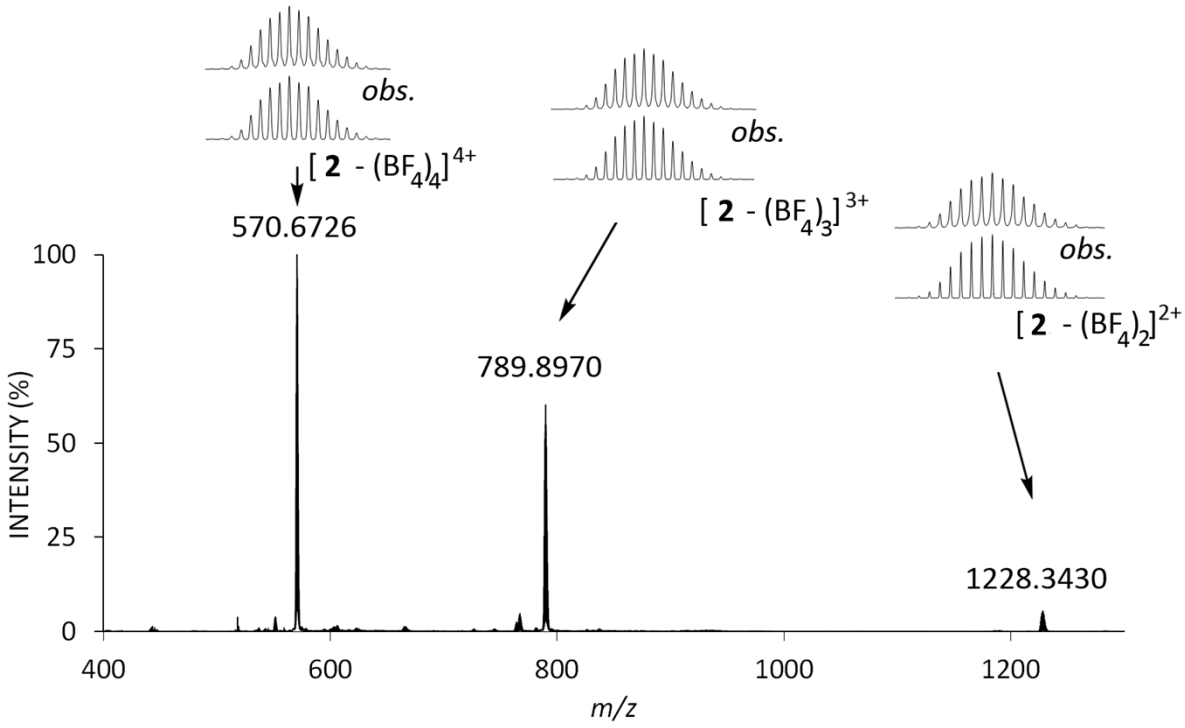

Figure 1.11 HR-ESMS (CH_3CN) of **2** with isotopic splitting patterns (observed shown above, calculated shown below).

2 Switching mechanism

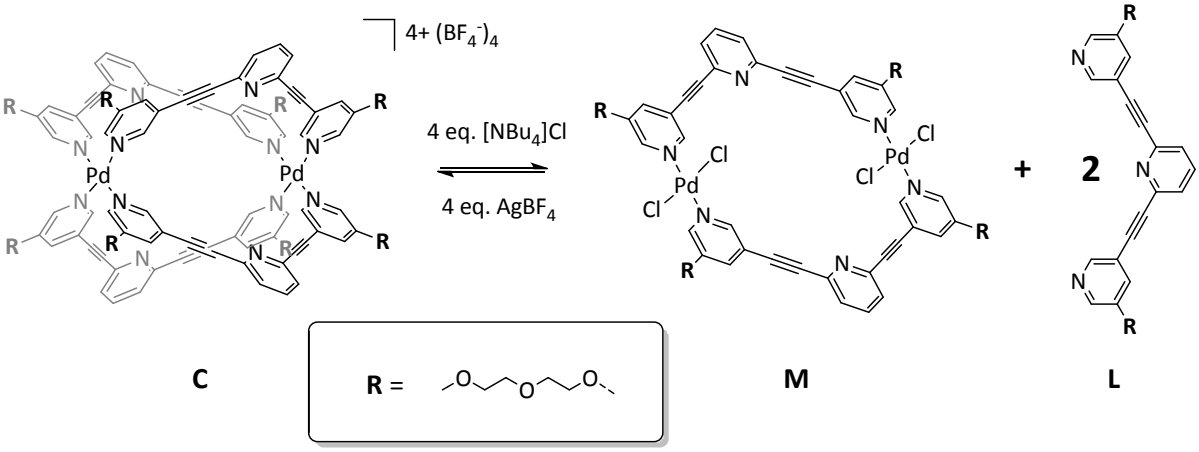

3 ^{1}H NMR stacked plot of mixed guest uptake and release

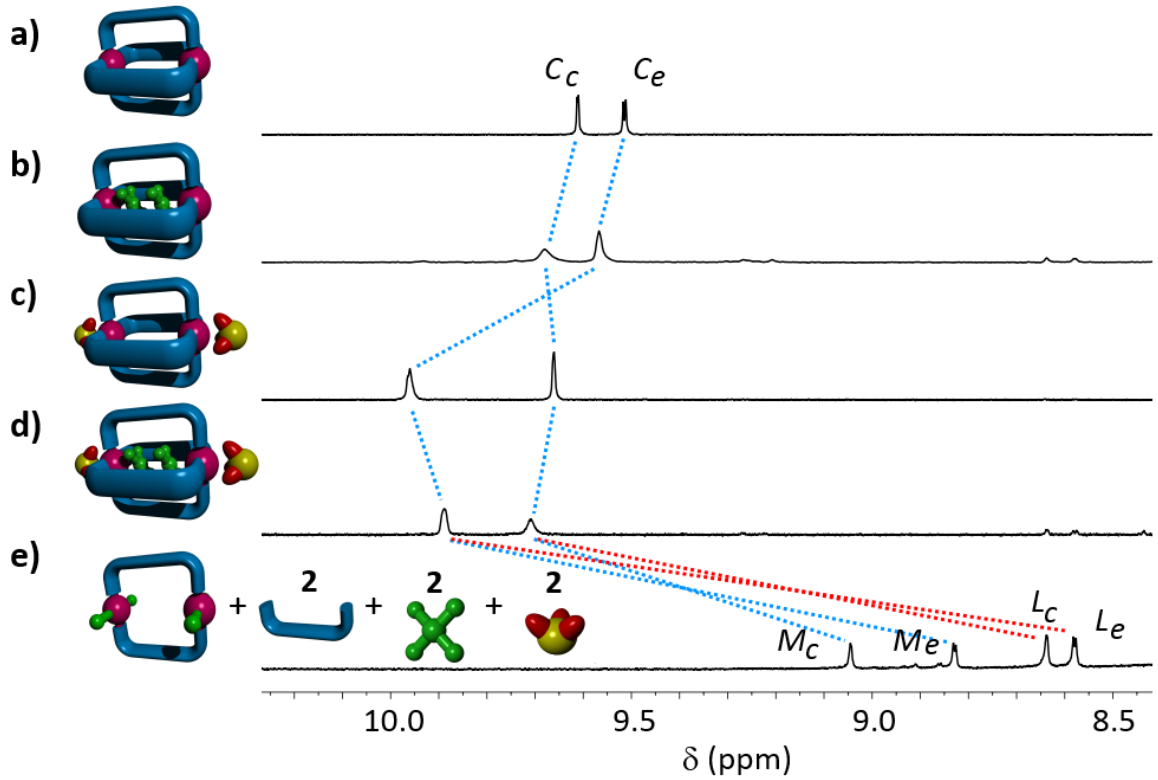

Figure 3.1 Partial stacked ^{1}H NMR specta (500 MHz, d_7-DMF, 298 K) of a) cage **C** (0.75 mM), b) addition of cisplatin to **C** giving [(cisplatin)$_2$⊂**C**]$^{4+}$ c) addition of [NBu$_4$](CH$_3$SO$_3$) to **C** giving [(MsO$^-$)$_2$⊂**C**]$^{2+}$, d) addition of cisplatin and [NBu$_4$](CH$_3$SO$_3$) to **C** giving [(cisplatin)$_2$(MsO$^-$)$_2$⊂**C**]$^{2+}$ and e) release of guests and formation of metallacycle **M** through addition of 4 equivalents of [NBu$_4$]Cl.

4 Binding studies

4.1 Mesylate

A series of ^{1}H NMR spectra (500 MHz, d_7-DMF, 298 K) were obtained in d_7-DMF (650 µL) of cage **C** (0.58 mM) in the presence of varying mole equivalents of $[NBu_4](CH_3SO_3)$. The change in chemical shift (Δδ) against zero equivalents of mesylate of proton H_e, the proton *ortho* to the coordinating nitrogen on the exterior face of the cage, was plotted against the number of equivalents, giving a plot consistent with binding capacity of two mesylate anions per cage, using the mole-ratio method.[2] Binding constants were obtained using a 2:1 binding isotherm, fitting experimental data to calculated values iteratively (K_1 = 1000 ± 100 M^{-1}, K_2 = 180 ± 20 M^{-1}).[3]

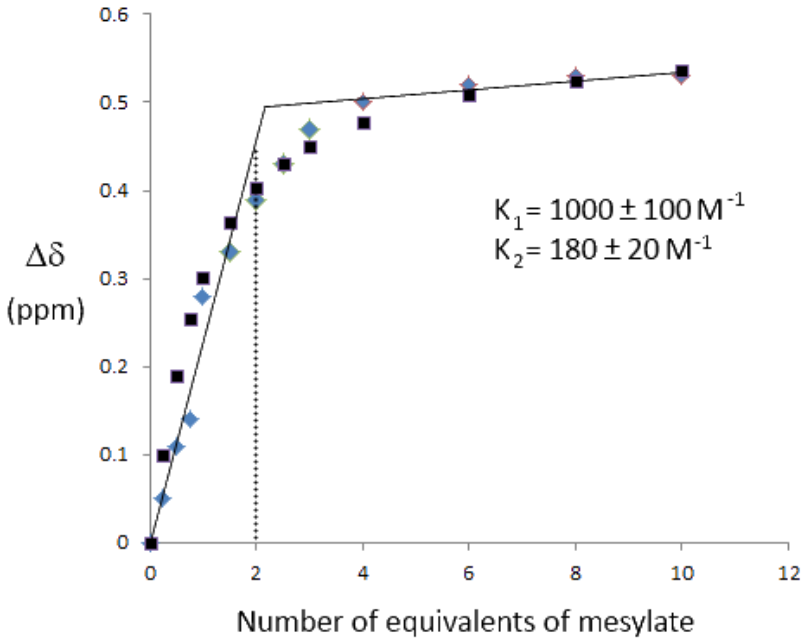

Figure 5.1 Plot of Δδ (ppm) of H_e (500 MHz, d_7-DMF, 298 K) against the number of equivalents of $[NBu_4](CH_3SO_3)$ per cage **C** (◆ observed, ■ calculated). The first linear trendline fitted through the first six data points (0, 0.25, 0.5, 0.75, 1.0 and 1.5 equivalents) and the second through the final four data points (4, 6, 8 and 10 equivalents).

4.2 Cisplatin

A series of ^{1}H NMR spectra (500 MHz, d_7-DMF, 298 K) were obtained in d_7-DMF (650 µL) of cage **C** (0.58 mM) in the presence of varying mole equivalents of cisplatin. The change in chemical shift (Δδ) against zero equivalents of cisplatin of proton H_e, the proton *ortho* to the coordinating nitrogen on the exterior face of the cage, was plotted against the number of equivalents. The changes in chemical shift were small and therefore the interaction was weak, but appeared sigmoidal in nature. Binding constants were obtained using a 2:1 binding isotherm, fitting experimental data to calculated values iteratively (K_1 = 2 $M^{-1} \pm 1$, K_2 = 5 $M^{-1} \pm 2$).[3]

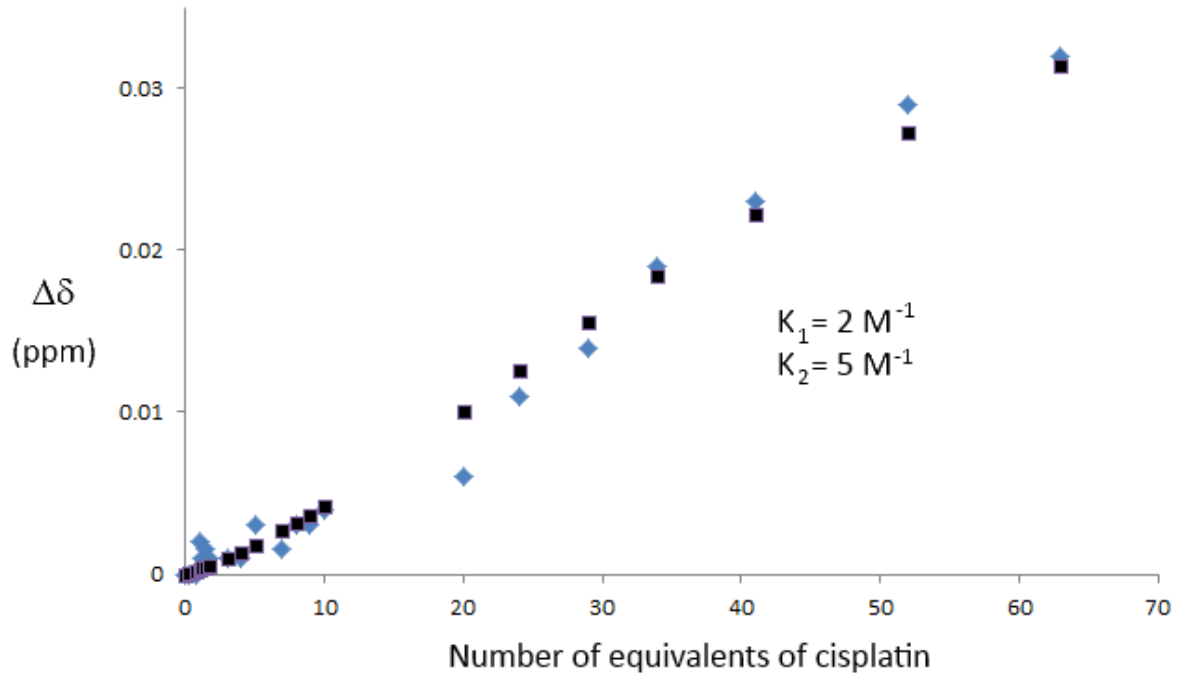

Figure 5.2 Plot of Δδ (ppm) of H_e (500 MHz, d_7-DMF, 298 K) against the number of equivalents of cisplatin per cage **C** (◆ observed, ■ calculated).

5 Molecular model of $[(\text{cisplatin})_2(\text{MsO}^-)_2 \subset \text{C}]^{2+}$

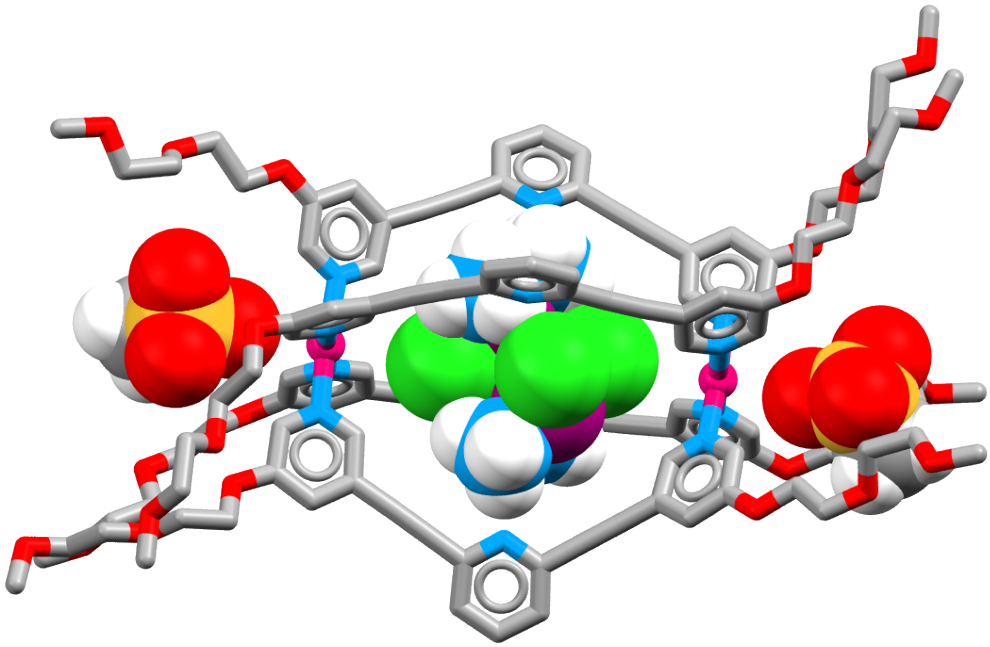

Figure 4.1 Energy minimised molecular model (SPARTAN '14) of $[(\text{cisplatin})_2(\text{MsO}^-)_2 \subset \mathbf{C}]^{2+}$, tube representation of **C** and spacefilling representation of guests.

6 ^{1}H DOSY NMR data

Table 5.1 ^{1}H DOSY NMR–derived diffusion coefficients (*D*) for compounds **C**, **M** and **L** (500 MHz, d_7-DMF, 298 K).

Compound	Diffusion coefficient (*D*) x 10^{-10} m^2 s^{-1}
C	2.16
M	3.10
L	4.56

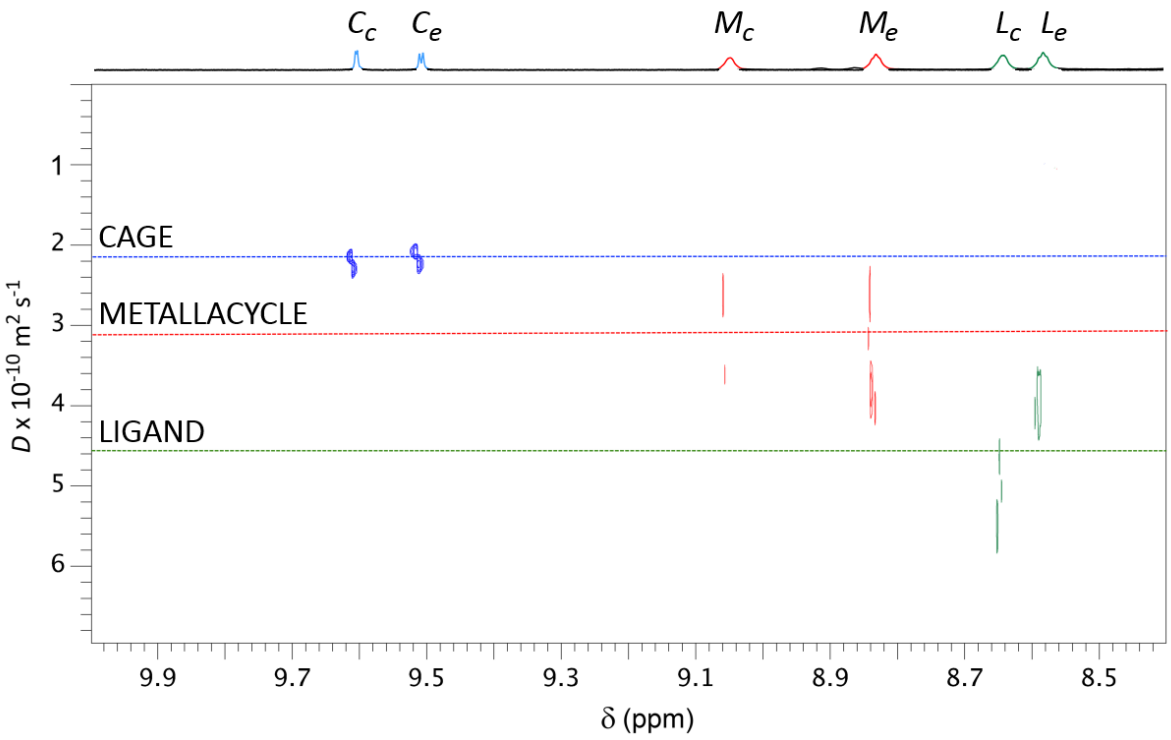

Figure 6.1 Overlaid partial ^{1}H DOSY NMR spectra (500 MHz, d_7-DMF, 298 K) showing diffusion of **C** (blue), **M** (red), and **L** (green).

7 X-ray data

7.1 Ligand L

An aqueous solution of **L** was allowed to evaporate, giving colourless needle-shaped crystals of **L**. X-ray data were collected at 100 K on an Agilent Technologies Supernova system using Cu Kα radiation with exposures over 1.0°, and data were treated using CrysAlisPro[4] software. The structure was solved using SIR-97[5] and weighted full-matrix refinement on F^2 was carried out using SHELXL-2013[6] running within the WinGX[7] package. All non-hydrogen atoms were refined anisotropically. Hydrogen atoms were placed in calculated positions and refined using a riding model.

The structure was solved in the monoclinic space group $P2_1/c$ and refined to an R_1 value of 4.1%. Present in the asymmetric unit is a molecule of ligand **L**.

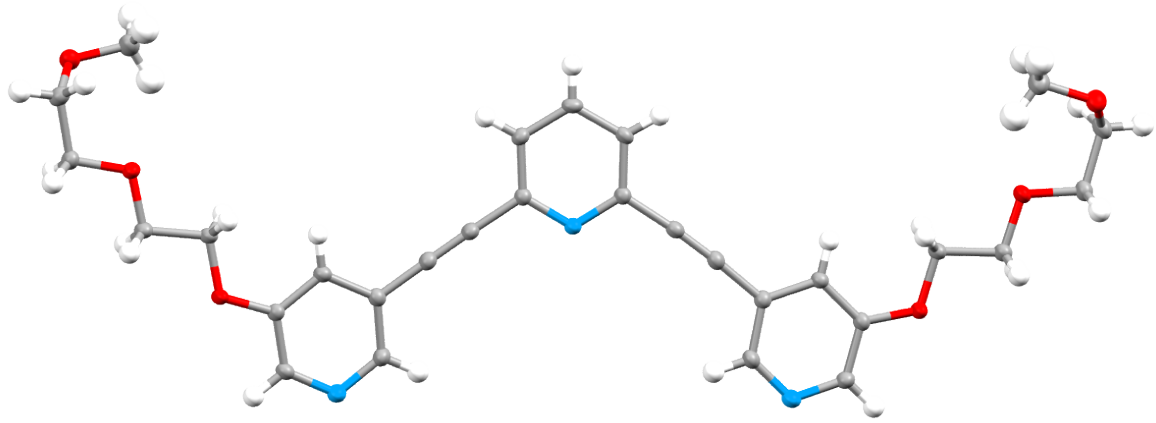

Figure 7.1 Ellipsoid Mercury representation of the asymmetric unit of **L**. Ellipsoids shown at 50% probability level.

7.2 Cage $[(H_2O)_4 \subset C](BF_4)_4$

A mixture of diethyl ether and an acetonitrile solution of **C** was shaken violently. The mixture was allowed to stand at room temperature overnight and gave yellow crystals of $[(H_2O)_4 \subset C](BF_4)_4$. X-ray data were collected at 100 K on an Agilent Technologies Supernova system using Cu Kα radiation with exposures over 1.0°, and data were treated using CrysAlisPro[4] software. The structure was solved using SIR-97[5] and weighted full-matrix refinement on F^2 was carried out using SHELXL-97[6] running within the WinGX[7] package. All non-hydrogen atoms were refined anisotropically. Hydrogen atoms attached to carbon atoms were placed in calculated positions and refined using a riding model. Hydrogen atoms attached to oxygen atoms were placed in calculated positions and orientated with sensible hydrogen-bonding acceptors.

The structure was solved in the triclinic space group $P\bar{1}$ and refined to an R_1 value of 7.5%. Present in the asymmetric unit is half of a $\mathbf{C}^{4+}$ cation, two BF_4^- anions and four solvent water molecules (each with 50% occupancy), encapsulated in the $\mathbf{C}^{4+}$ cation.

One of the BF_4^- anions was disordered and modelled with the PART command with occupancies of 60% (B2 and F5 to F8) and 40% (B3 and F9 to F12) over two sites. The minor component was modelled with the SAME command. The two solvent water molecules were disordered and modelled

with the PART command with occupancies of 50% over two sites. The DFIX command was used to fix all O-H distances in solvent water molecules to 0.85 Å. The ISOR command was applied to solvent water oxygen atoms O50 and O51.

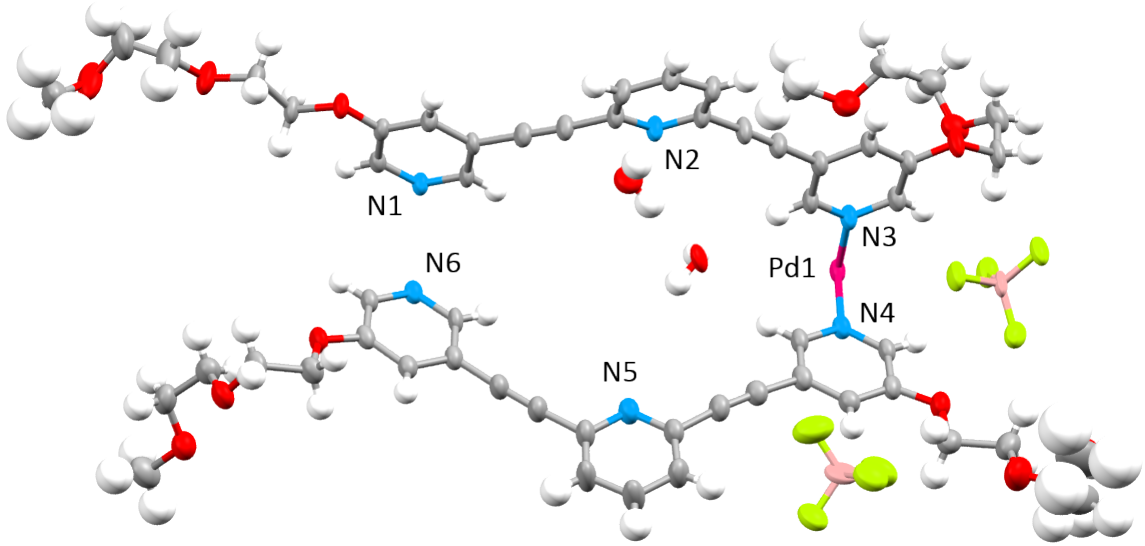

Figure 7.2 Ellipsoid Mercury representation of the asymmetric unit of $[(H_2O)_4 \subset \mathbf{C}](BF_4)_4$. Ellipsoids shown at 50% probability level.

The crystal lattice contained a small amount of diffuse electron density (outside the cavity of the $\mathbf{C}^{4+}$ cation) that could not be appropriately modelled. The SQUEEZE routine within PLATON was employed to resolve this problem, resulting in void electrons count of 17 that was assigned to two solvent water molecules (16 electrons in total).

Table 6.1 SQUEEZE results for $[(H_2O)_4 \subset \mathbf{C}](BF_4)_4$.

Platon squeeze void number	1	2
Platon squeeze void average x	0.264	0.736
Platon squeeze void average y	0.877	0.122
Platon squeeze void average z	0.595	0.405
Platon squeeze void volume	26.1	26.1
Platon squeeze void count electrons	9.2	8.2
Platon squeeze details	Solvent water molecules that could not be appropriately modelled	

In the crystal structure of $[(H_2O)_4 \subset \mathbf{C}](BF_4)_4$, one of the BF_4^- counterions was cradled in the diglyme chains above the palladium ion on the exterior of the cage, aligned such that fluoride atom (F4) was pointed towards the palladium ion (Fig 3.3). This fluoride atom was involved in quadfurcated hydrogen bonding to the four exohedral H_e protons (hydrogen bonding distances from 2.179(4) to 2.665(5) Å) as well as interaction with the metal (a Pd – F distance of 3.088(5) Å).

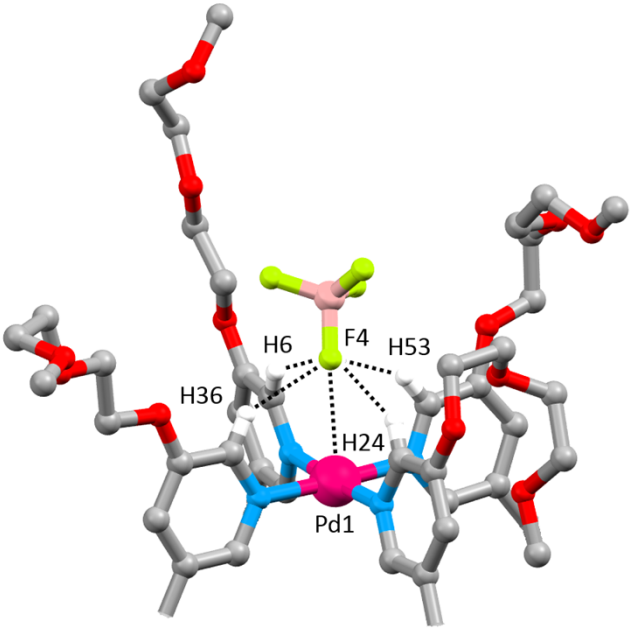

Figure 7.3 Partial ball and stick model of the crystal structure of $[(H_2O)_4 \subset \mathbf{C}](BF_4)_4$, showing interactions between the fluoride F4 of a BF_4^- counterion and exohedral pyridyl protons and the palladium(II) centre. All hydrogen atoms except H6, H36, H24 and H53 omitted for clarity. Selected distances (Å): Pd1·····F4 3.088(5), H6·····F4 2.665(5), H24·····F4 2.179(4), H36·····F4 2.306(4), H53·····F4 2.541(3).

7.3 Metallacycle M

Vapour diffusion of diethyl ether into a solution of **C** in DMF in the presence of a chloride source gave yellow crystals of **M**. X-ray data were collected at 100 K on an Agilent Technologies Supernova system using Cu Kα radiation with exposures over 1.0°, and data were treated using CrysAlisPro[4] software. The structure was solved using SIR-97[5] and weighted full-matrix refinement on F^2 was carried out using SHELXL-97[6] running within the WinGX[7] package. All non-hydrogen atoms were refined anisotropically. Hydrogen atoms attached to carbon atoms were placed in calculated positions and refined using a riding model.

The structure was solved in the monoclinic space group $C2/m$ and refined to an R_1 value of 5.52%. Present in the asymmetric unit is one quarter of the metallacycle: consisting of half of ligand **L**, and half of one palladium(II) cation bound to two chloride atoms.

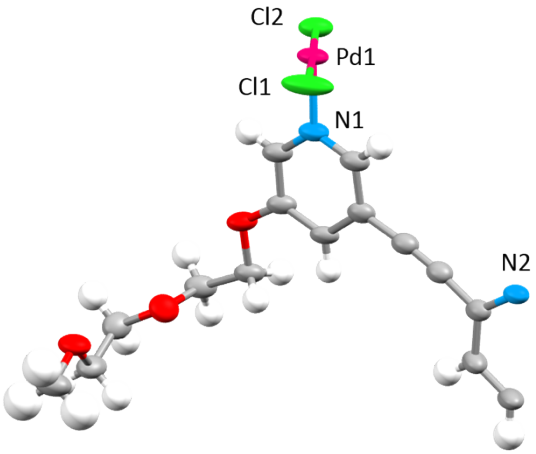

Figure 7.4 Ellipsoid Mercury representation of the asymmetric unit of **M**. Ellipsoids shown at 50% probability level.

The crystal lattice contained a large amount of diffuse electron density that could not be appropriately modelled. The SQUEEZE routine within PLATON was employed to resolve this problem, resulting in void electrons count of 116 that was assigned to two solvent DMF molecules and three water molecules (110 electrons in total).

Table 6.2 SQUEEZE results for **M**.

Platon squeeze void number	**1**	**2**	**3**	**4**	**5**	**6**
Platon squeeze void average x	0.000	0.500	0.165	0.665	0.335	0.835
Platon squeeze void average y	0.000	0.500	0.500	0.000	0.000	0.500
Platon squeeze void average z	-0.006	0.016	0.475	0.475	0.525	0.525
Platon squeeze void volume	145	145	25	25	25	25
Platon squeeze void count electrons	54	54	2	2	2	2
Platon squeeze details	Solvent DMF molecules and water molecules that could not be appropriately modelled					

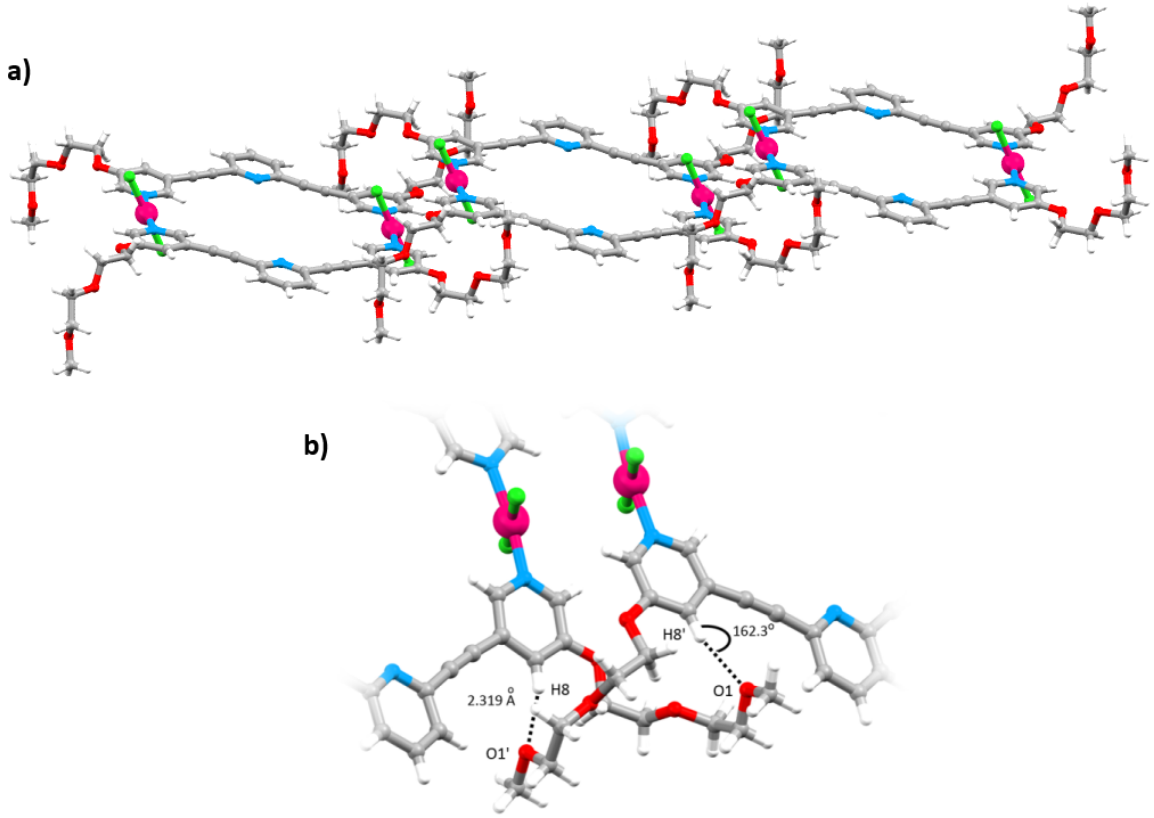

Figure 7.5 Ball and stick Mercury representation of a) stepwise packing of metallacycle **M**, b) non-classical hydrogen bonding exists between the terminal ether oxygen (O1) and the C-H *para* to the coordinating nitrogen (H8).

7.4 Cage $[(DMF)_2(MsO^-)_2 \subset C](MsO^-)_2$

Cage **C** was combined with ten equivalents of $[NBu_4](CH_3SO_3)$ in d_7-DMF. Vapour diffusion of diethyl ether into the solution gave colourless block crystals of $[(DMF)_2(MsO^-)_2 \subset$ **C**$](MsO^-)_2 \cdot 2DMF$. X-ray data were collected at 100 K on an Agilent Technologies Supernova system using Mo Kα radiation with exposures over 1.0°, and data were treated using CrysAlisPro[4] software. The structure was solved using SIR-2011[5] and weighted full-matrix refinement on F^2 was carried out using SHELXL-97[6] running within the WinGX[7] package. All non-hydrogen atoms were refined anisotropically. Hydrogen atoms attached to carbon atoms were placed in calculated positions and refined using a riding model, or fixed in sensible geometries where necessary.

The structure was solved in the monoclinic space group $P2_1/n$ and refined to an R_1 value of 10.86%. Present in the asymmetric unit is one half of a cage (two of ligand **L**, and one Pd(II) centre), two mesylate counterions, and two DMF solvent molecules, one within the cavity and the other outside.

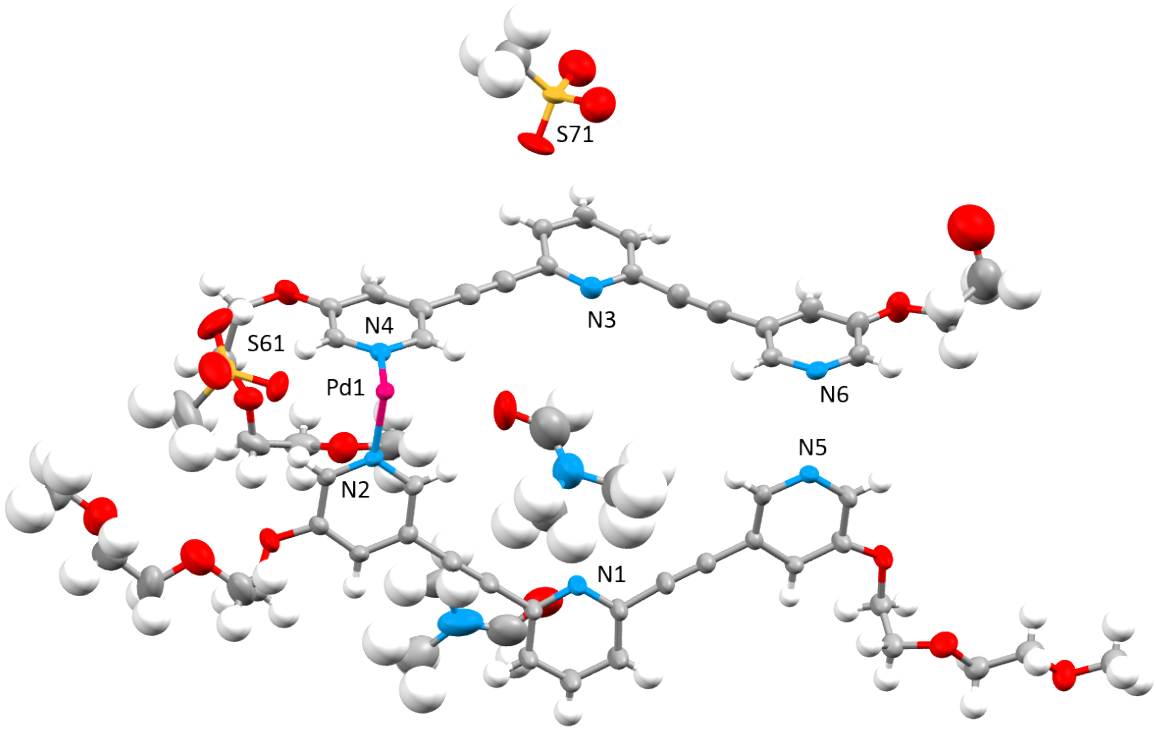

Figure 7.6 Ellipsoid Mercury representation of the asymmetric unit of $[(DMF)_2(MsO^-)_2 \subset \mathbf{C}](MsO^-)_2 \cdot 2DMF$. Ellipsoids shown at 50% probability level.

The mesylate anion containing S71 was disordered and was modelled using the DFIX command for all constituent non-hydrogen atoms and the ISOR command for C71, O72 and O73. The encapsulated DMF solvent molecule was also disordered and was modelled using the ISOR command for C91, C92 and C93. One of the diglyme chains in the asymmetric unit (two per cage) was disordered. The disorder could not be resolved through parting, or from using the predominant Q-peaks and then squeezing. In addition, the terminal methyl group could not be located nor placed in a sensible position. Accordingly, the final eleven atoms in the chain ($CH_2CH_2OCH_3$) were not included in the structure and the SQUEEZE routine within PLATON was employed to resolve the problem of residual electron density, resulting in void electrons count of 364 that was assigned to the four missing chain ends (132 electrons), four DMF solvent molecules (160 electrons) and six water molecules (60 electrons) for a total of 352 electrons. The values of both the weighted *R* factor and wR_2 were high (0.380 for both), giving B alerts in the cif check.

Table 6.3 SQUEEZE results for $[C\subset(DMF)_2(MsO^-)_2](MsO^-)_2\cdot 2DMF$.

Platon squeeze void number	**1**	**2**	**3**	**4**	**5**	**6**
Platon squeeze void average x	0.000	0.082	-0.082	0.500	0.418	0.582
Platon squeeze void average y	0.000	0.730	0.270	0.500	0.230	0.770
Platon squeeze void average z	0.000	0.357	0.643	0.500	0.143	0.857
Platon squeeze void volume	288	73	73	288	73	73
Platon squeeze void count electrons	55	18	18	55	18	18
Platon squeeze details	Solvent DMF molecules, water molecules and diglyme chain subsitutents that could not be appropriately modelled					

The largest Q-peak, Q1, together with Q6 and Q7, located within an area of electron density possibly consisting of an unresolved DMF molecule. Q2, Q3 and Q5 located around the mesylate counterion not bound to the exohedral palladium face. Q4 is located within the region where the diglyme chain could not be appropriately modelled.

The internal cavity of the cage is inhabited by two symmetry equivalent solvent DMF molecules. Two symmetry equivalent mesylate anions are cradled in the diglyme chains on the exohedral face of the palladium(II) centres.

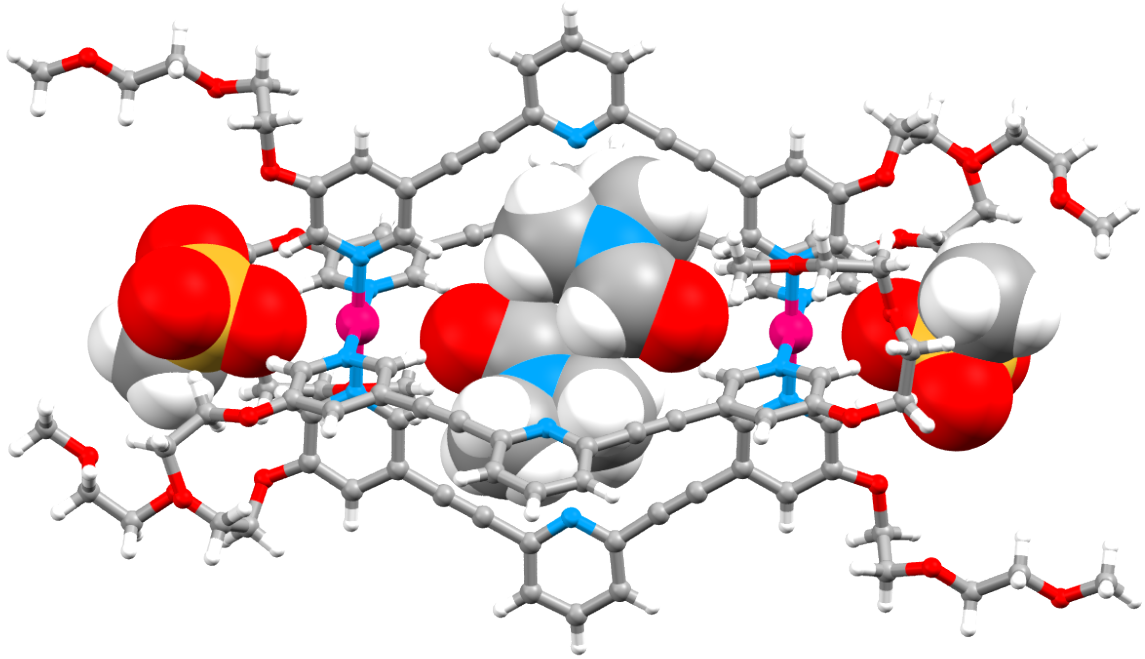

Figure 7.7 Ball and stick Mercury representation of cage $[Pd_2\mathbf{L}_4]^{4+}$ with spacefilling representation of two DMF solvent molecules and two mesylate anions bound endohedrally and exohedrally respectively.

The oxygen on the mesylate anion directed towards the palladium (O61) is involved in quadfurcated non-classical hydrogen bonding to the four exohedral protons *ortho* to the coordinating nitrogen atoms (H9, H26, H42 and H53), and an interaction with the palladium(II) metal.

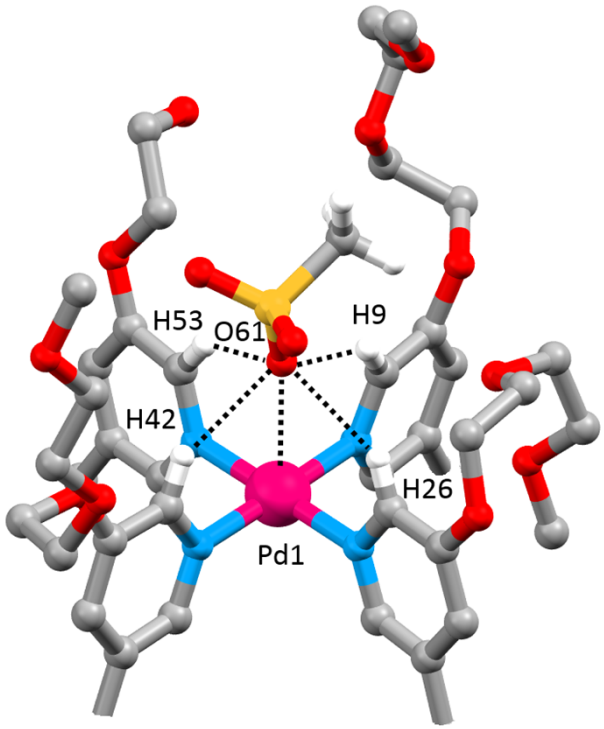

Figure 7.8 Partial ball and stick model of the crystal structure of $[(DMF)_2(MsO^-)_2\subset\mathbf{C}](MsO^-)_2\cdot 2DMF$.showing interactions between O61 of a mesylate, and exohedral pyridinyl protons or the palladium(II) centre. Some hydrogen atoms omitted for clarity; H9, H26, H42 and H53 shown. Selected distances (Å): Pd1·····O61 2.886(4), H9·····O61 2.295, H26·····O61 2.493, H42·····O61 2.275, H53·····O61 2.499.

7.5 Crystallographic data

Identification code	Ligand L		Cage $[(H_2O)_4 \subset C](BF_4)_4$	
Empirical formula	$C_{29}\ H_{31}\ N_3\ O_6$		$C_{116}\ H_{132}\ B_4\ F_{16}\ N_{12}\ O_{28}\ Pd_2$	
Formula weight	517.57		2702.38	
Temperature	100.0(2) K		100.0(1) K	
Wavelength	1.54184 Å		1.54184 Å	
Crystal system	Monoclinic		Triclinic	
Space group	$P\ 2_1/c$		$P\bar{1}$	
Unit cell dimensions	a = 19.2486(2) Å	α= 90°	a = 14.8562(5) Å	α= 117.401(3)°
	b = 10.91640(10) Å	β= 93.1170(10)°	b = 16.5839(5) Å	β= 93.110(2)°
	c = 12.41140(10) Å	γ = 90°	c = 16.9982(4) Å	γ = 114.691(3)°
Volume	2604.09(4) Å^3		3216.53(16) Å^3	
Z	4		1	
Density (calculated)	1.320 Mg/m^3		1.395 Mg/m^3	
Absorption coefficient	0.763 mm^{-1}		3.098 mm^{-1}	
F(000)	1096		1392	
Crystal size	0.27 x 0.22 x 0.09 mm^3		0.24 x 0.09 x 0.05 mm^3	
Theta range for data collection	4.60 to 76.78°		3.08 to 76.54°	
Index ranges	-23<=h<=24, -13<=k<=13, -15<=l<=11		-18<=h<=18, -20<=k<=20, -19<=l<=21	
Reflections collected	40606		39257	
Independent reflections	5459 [$R_{(int)}$ = 0.0409]		13327 [$R_{(int)}$ = 0.0675]	
Completeness	100.00% to theta = 67.00°		100.00% to theta = 77.03°	
Absorption correction	Gaussian		Gaussian	
Max. and min. transmission	0.987 and 0.966		0.890 and 0.679	
Refinement method	Full-matrix least-squares on F_2		Full-matrix least-squares on F_2	
Data / restraints / parameters	5459 / 0 / 345		13327 / 30 / 869	
Goodness-of-fit on F2	1.098		1.121	
Final R indices [I>2sigma(I)]	R_1 = 0.0413, wR_2 = 0.1046		R_1 = 0.0749, wR_2 = 0.2070	
R indices (all data)	R_1 = 0.0444, wR_2 = 0.1066		R_1 = 0.1015, wR_2 = 0.2251	
Largest diff. peak and hole	0.267 and -0.238 e.Å^{-3}		3.169 and -0.882 e.Å^{-3}	

Identification code	Metallacycle M		[(DMF)$_2$(MsO$^-$)$_2$⊂C](MsO$^-$)$_2$·2DMF.	
Empirical formula	C_{58} H_{62} Cl_4 N_6 O_{12} Pd_2		C_{126} H_{150} N_{16} O_{38} Pd_2 S_4	
Formula weight	1389.74		2837.66	
Temperature	100.01(10) K		100.01(10) K	
Wavelength	1.54184 Å		0.71073 Å	
Crystal system	Monoclinic		Monoclinic	
Space group	*C*2/*m*		*P*1 2_1/*n* 1	
Unit cell dimensions	a = 13.8958(6) Å	α= 90°	a = 13.099 Å	α= 90°
	b = 21.0537(7) Å	β= 101.982(4)°	b = 17.179 Å	β= 91.566(2)°
	c = 11.1192(5) Å	γ = 90°	c = 32.2500(10) Å	γ = 90°
Volume	3182.1(2) Å^3		7254.4(2) Å^3	
Z	2		2	
Density (calculated)	1.450 Mg/m^3		1.299 Mg/m^3	
Absorption coefficient	6.618 mm^{-1}		0.384 mm^{-1}	
F(000)	1416		2956	
Crystal size	0.17 x 0.13 x 0.08 mm^3		0.33 x 0.19 x 0.16 mm^3	
Theta range for data collection	3.87 to 76.32°		2.90 to 26.02°	
Index ranges	-11<=h<=17, -26<=k<=26, -11<=l<=13		-14<=h<=16, -21<=k<=21, -39<=l<=39	
Reflections collected	7617		105476	
Independent reflections	3299 [$R_{(int)}$ = 0.0258]		14267 [$R_{(int)}$ = 0.0381]	
Completeness	98.80% to theta = 67.00°		99.80% to theta = 26.02°	
Absorption correction	Gaussian		Gaussian	
Max. and min. transmission	1.00000 and 0.47054		1.00000 and 0.63630	
Refinement method	Full-matrix least-squares on F_2		Full-matrix least-squares on F_2	
Data / restraints / parameters	3299 / 0 / 191		14267 / 58 / 838	
Goodness-of-fit on F2	1.086		1.86	
Final R indices [I>2sigma(I)]	R_1 = 0.0552, wR_2 = 0.1589		R_1 = 0.1103, wR_2 = 0.3733	
R indices (all data)	R_1 = 0.0627, wR_2 = 0.1674		R_1 = 0.1201, wR_2 = 0.3871	
Largest diff. peak and hole	2.795 and -1.107 e.Å^{-3}		4.230 and -1.480 e.Å^{-3}	

8 References

[1] V. Gudipati, D. P. Curran, C. S. Wilcox, *J. Org. Chem.* **2006**, *71*, 3599-3607.

[2] A. S. Meyer, Jr., G. H. Ayres, *J. Am. Chem. Soc.* **1957**, *79*, 49-53.

[3] R. D. Sommer, A. L. Rheingold, A. J. Goshe, B. Bosnich, *J. Am. Chem. Soc.* **2001**, *123*, 3940-3952.

[4] CrysAlisPro; Agilent Technologies: Yarnton, England, 2012.

[5] A. Altomare, M. C. Burla, M. Camalli, G. L. Cascarano, C. Giacovazzo, A. Guagliardi, A. G. G. Moliterni, G. Polidori, R. Spagna, *J. Appl. Cryst.* **1999**, *32*, 115-119.

[6] G. Sheldrick, *Acta Cryst.* **2008**, *A64*, 112-122.

[7] L. Farrugia, *J. Appl. Cryst.* **1999**, *32*, 837-838.